



Tailoring Anisotropy and Heterogeneity of Selective Laser Melted Ti6Al4V Alloys

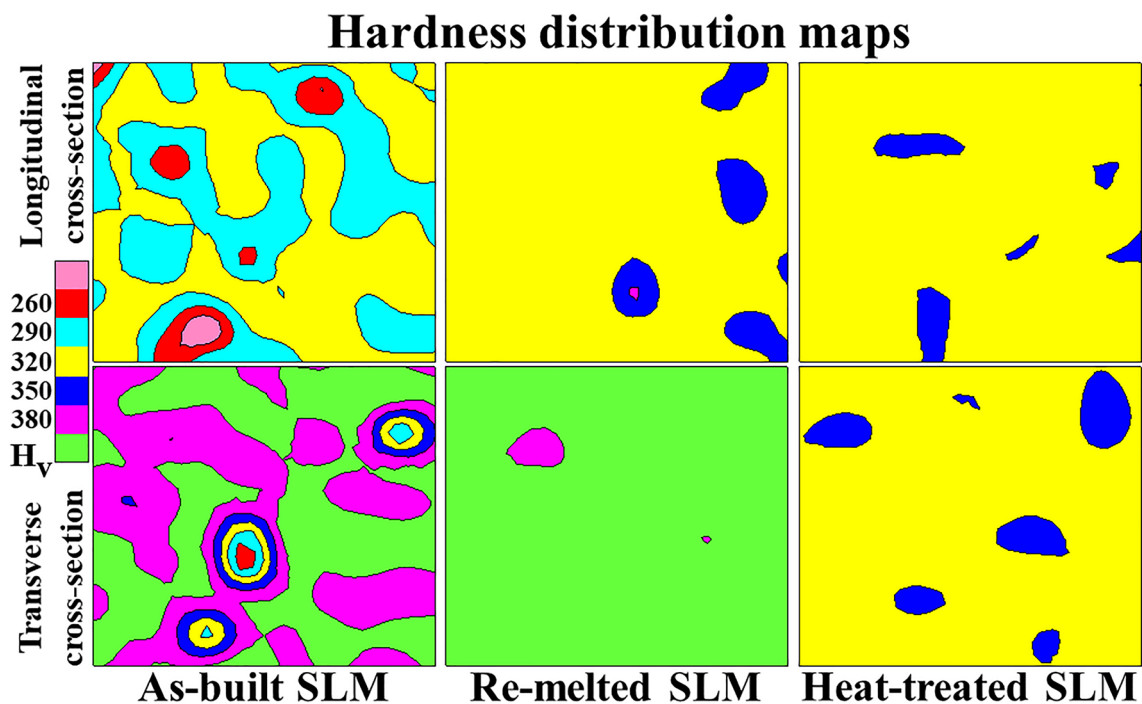
J. Karimi^{1,2} · L. Kollo¹ · K. G. Prashanth^{1,3,4}

Received: 16 November 2022 / Accepted: 10 February 2023 / Published online: 19 February 2023
© Indian National Academy of Engineering 2023

Abstract

Selective laser melting (SLM) provides an opportunity to manufacture parts with complex geometry, minimal wastage, and no need for special tooling. However, the fabricated parts exhibit heterogeneity and anisotropy in mechanical properties and residual stresses, which have been long-term concerns of the SLM of metallic materials. The present study investigates the effect of melting sequence and heat treatment on such heterogeneous and anisotropic properties in the SLM Ti6Al4V alloys. As a relatively low-cost and effective approach, the application of melting sequence led to the homogenization of the microstructure and improvement of mechanical properties, though anisotropy in properties (residual stresses, hardness) remained. The application of the heat treatment process not only homogenized the hardness but also reduced the anisotropy. These approaches would be considered as the two potential strategies to overcome the shortcoming of the SLM process, depending on the required properties, possibility and performance, and the budget.

Graphical abstract



Keywords Additive manufacturing · Selective laser melting · Laser remelting · Anisotropy · Heterogeneity · Heat treatment

Extended author information available on the last page of the article

Introduction

Additive manufacturing (AM) technologies can be used in a wide range of applications in various industries, such as automotive, aerospace, transportation, medical, and energy. The selective laser melting (SLM) process is considered to be a superior additive manufacturing process that has the capability of producing complex objects with high geometrical accuracy, low material waste, and short total manufacturing time. Although there are a countless number of studies that have clearly stated the advantages of SLM (Vrancken et al. 2012; Rahmani et al. 2019, 2020; Karimi et al. 2020), there are still some shortcomings in obtaining homogeneous phase microstructure and isotropic mechanical properties. Recent reports demonstrate that the mechanical properties and microstructure of SLM improved by heat treatment (Wang et al. 2016) and pre-heating of powder bed (Ali et al. 2017). However, there is a lack of approach to produce parts by SLM with isotropic and homogeneous microstructure and mechanical properties without external post-treatment processes, which will reduce efficiency and increase manufacturing time.

Ti6Al4V alloys, which were introduced in 1954 in the USA, are an $\alpha + \beta$ titanium alloy with high specific strength, low density, desirable tribological properties, high fracture toughness, excellent corrosion resistance, and superior biocompatibility. Ti6Al4V alloys are the most popular titanium alloys used in several industries and occupy almost half of the market share of titanium products used in the world today. Ti6Al4V exhibits an alpha–beta phase, depending on the microstructure and, subsequently, the thermal processing of the material. In the cooling rate (above 410 K/s), the α' martensite phase is formed, which shows superior mechanical properties as compared with those of the alpha–beta phase. A slow cooling rate from above the β transus temperature results in the formation of globular α (Karimi et al. 2022). This low-density and strong alloy saves weight in highly loaded structures; hence, it is extremely suitable for jet engines, gas turbines, and many airframe components.

In the SLM process, the material undergoes rapid heating and solidification, and the high velocity of the melt pool front is induced by the laser beam velocity. The SLM parts are subject to a complex cyclic thermal history, including directional heat extraction and repeated heating during layer-by-layer manufacturing. The whole thermal history between solidification and cooling down to room temperature in a very short time leads to heterogeneous and anisotropic microstructure and mechanical properties of the parts produced using the SLM process (Vrancken et al. 2014; Karimi 2022; Zheng et al. 2022). Melting sequence (remelting) is a non-additive technique

that utilizes a laser beam to impart energy to remelt the material. This strategy could reduce heterogeneity and anisotropy of the additively manufactured parts (Karimi 2022). Various process parameters, including the number of remelting, scanning speed, laser power, and laser speed along with the scanning strategy, can be applied during the melting sequence strategy. In addition, a partially or fully remelting strategy can be used to fabricate SLM parts and influence the microstructural and mechanical properties. Several studies have investigated the effect of partial remelting on the SLM components and reported that this strategy has a significant impact on surface quality (Pantelejev et al. 2016; Karimi et al. 2021b). Yasa and Kruth (2011) reported a significant reduction in the surface roughness of the SLMed parts with melting sequence strategy, from ~ 15 to ~ 2 μm . Many studies have reported improving the density of the SLM part with the application of melting sequence (Vaithilingam et al. 2016; Shiomi et al. 2004; Karimi 2022; Ali et al. 2018). On the other hand, little literature gives a comparative analysis of the effect of this approach on heterogeneity in microstructure and anisotropy in the mechanical properties so far. The melting sequence strategy increases production costs and time. However, this strategy can be an alternative approach to tailor the microstructure and mechanical properties of the SLM components. The melting sequence strategy can be used during in situ alloying via SLM from elemental powders, which could eliminate the inhomogeneous distribution of the mixed elements (Karimi 2022). Nevertheless, there is a lack of comparative study of the effect of the heat treatment process and the melting sequence strategy on the heterogeneity and anisotropy of the SLM parts. Accordingly, the melting sequence was explored as an approach to minimize the anisotropy and heterogeneity, and the results were compared with the heat treatment approach.

Experimental Methods

A Realizer SLM50 equipped with a 120 W Yb-fiber laser with a wavelength of ~ 1.07 μm was applied to fabricate Ti6Al4V specimens from gas-atomized powder with a layer thickness of 0.025 mm, a hatch distance of 0.06 mm, and a scan speed of 1000 mm/s. Each layer of the Ti6Al4V powder particles was melted either once or three times using the same process parameters to study the influence of the laser re-scanning strategy. SLM samples were fabricated with different melting sequences, and the result of single and triple melting was reported here, which showed a distinct difference in the mechanical properties. The structural characterization was analyzed using X-ray diffractometer Rigaku SmartLab SE with a D/teX Ultra 250 1D detector equipped with Cu-K α radiation. The measurements were conducted at

room temperature (23 °C) from 20 to 120° (2 θ) with a 0.04° step size. Chemical composition was characterized by transmission electron microscopy (Tecnai G2 F20) coupled with energy-dispersive X-ray spectroscopy. In seven angles, residual stress was measured using an Asenware AW-XDM300 (HAOYUAN) X-ray diffraction (XRD) in seven angles ϕ (0°, 15°, 30°, 45°, -10°, -20°, and -30°). The microstructure was examined by scanning electron microscopy (SEM) using a Zeiss FEG microscope. The dimensions of the acicular α/α' were determined with 150 measurements. The microhardness test was carried out over 100 indents on each surface using a MICROMET 2001 with a force of 200 g and a dwell time of 10 s. Compression tests were conducted on a servo hydraulic Instron 8516. Particle size distribution was measured using HORIBA LA-950. The heat treatment of as-SLM was conducted in a vacuum furnace above the β transus

(~995 °C) at 1100 °C for 3 h, and cooled inside the furnace. Various heat treatment temperatures were examined, and those that were heat treated above the β transus temperature. It is worth to mention that several works heat-treated AMed Ti6Al4V above β transus temperature (Vrancken et al. 2012; Fidan et al. 2013; Srinivasan et al. 2022).

Results and Discussion

The XRD pattern of the gas-atomized Ti6Al4V powder is shown in Fig. 1a, which exhibits a single-phase hcp α -Ti. The inset shows the morphology of powder particles, which are spherical in shape, and some satellite particles are attached to them. Figure 1b shows the distribution and cumulative volume fraction of powder particle sizes. It can

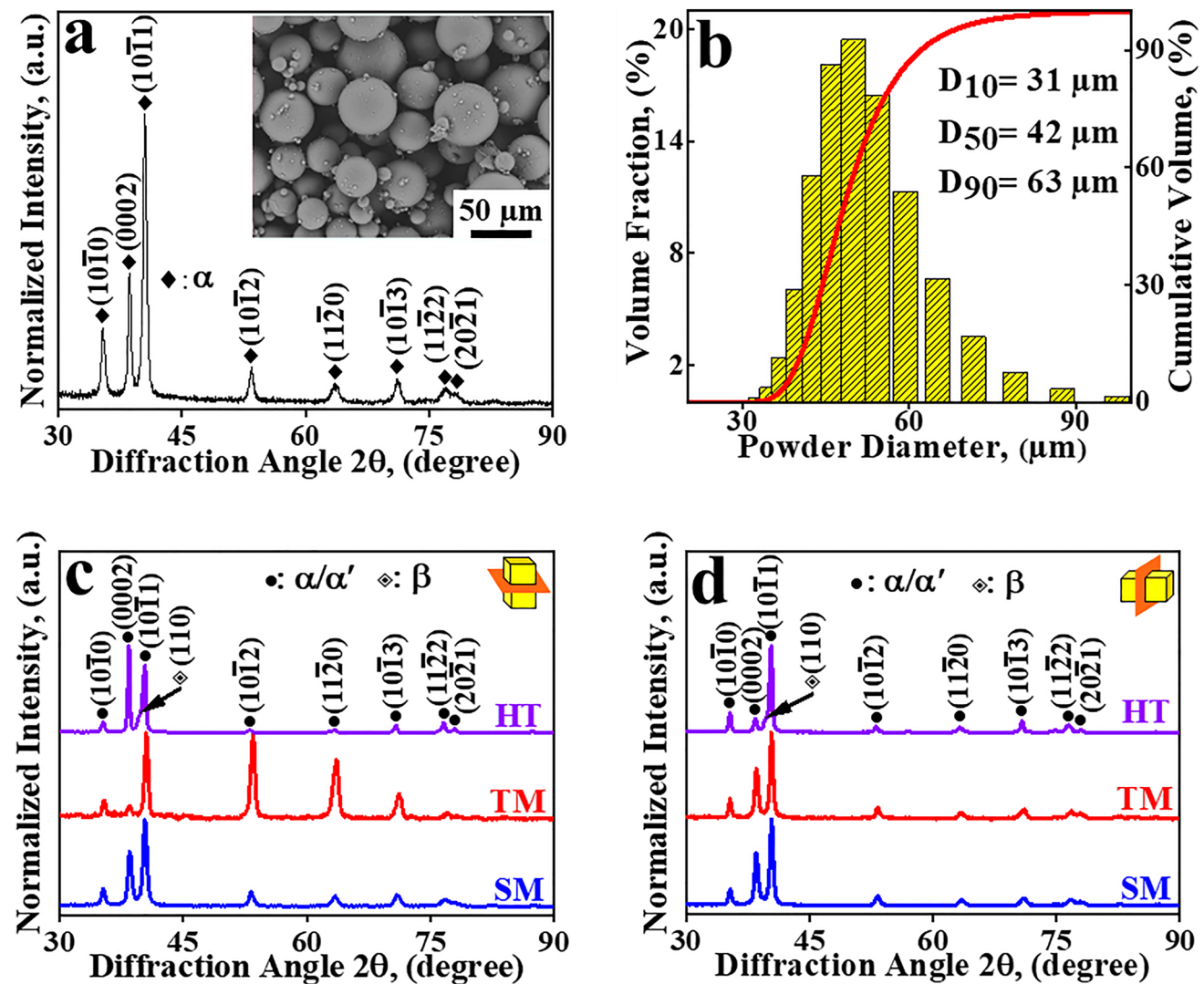


Fig. 1 **a** XRD pattern, and **b** size distribution of the Ti6Al4V powder. The inset shows the SEM micrograph of the powder. XRD patterns of the SLM samples: **c** TCS and **d** LCS

be seen that the powder consists of a narrow range of particle sizes ($D_{10} \sim 31$ and $D_{90} \sim 63 \mu\text{m}$), and the median size was observed to be $\sim 42 \mu\text{m}$. The XRD of the SLM samples, including single melting (SM), triple melting (TM), and heat-treated (HT) samples, in the transverse cross-section (TCS) and longitudinal cross-section (LCS), are illustrated in Fig. 1c and Fig. 1d, respectively. The diffractograms of the SM and TM samples show the presence of α/α' phase in TCS and LCS. Compared to SM and TM samples, diffractograms of HT sample in both the TSC and LCS indicate the presence of β phase peaks (at 39.5°) because of the transformation of α/α' into $\alpha + \beta$ phases as a result of the heat treatment above β transus (995°C), as also noted by Vrancken et al. (2012).

The microstructure of the SM and TM samples in TCS and LCS consists of α/α' phase (Fig. 2a–d), corroborating the XRD results. The persistence of the fine needles in the fabricated SLM samples is attributed to the rapid solidification ($\sim 10^5^\circ\text{C/s}$). Although the acicular α' shape remains the same, its size in TCS and LCS changes with remeltings. Accordingly, the average distance between the acicular α' , λ , was measured. λ decreases from 1.8 ± 0.7 to $0.8 \pm 0.25 \mu\text{m}$ with increasing the melting sequence from SM to TM, respectively. On the other hand, the microstructure of the HT sample in both the TCS and LCS consists of $\alpha + \beta$ lamellar, in agreement with the XRD pattern (Fig. 2e, f).

Figure 2g illustrates the average Vickers hardness values of the samples in the TCS and LCS, where they increase from 323 ± 15 and $406 \pm 29 \text{H}_v$ for the SM sample to 338 ± 16 and $440 \pm 19 \text{H}_v$ for the TM sample, respectively. On the other hand, the average Vickers hardness of the HT sample in the TCS and LCS was observed to be 344 ± 8 and 340 ± 15 , respectively. The hardness of the SM and TM samples in the LCS is $\sim 30\%$ higher than the TCS, which is ascribed to the intrinsic anisotropy in mechanical properties of SLM because of the columnar grain growth along the building direction (Wu et al. 2016). However, the heat treatment process led to the reduction of such anisotropy. In addition, because of the very high-temperature gradients and rapid solidification, the residual stresses remain in the SLM parts, which may affect the mechanical and tribological properties. In our previous work (Karimi et al. 2021b), the effect of melting sequence on the inhomogeneity in the microstructure and the mechanical properties (fatigue and impact behaviors) of SLM Ti6Al4V alloys was investigated. The change in the number of melting steps could affect the microstructure of the fabricated parts. Remelting influenced the size of the acicular α' martensite dimensions, which subsequently led to the differences in the hardness.

The residual stresses of the TCS and LCS increased from 348 and 722 MPa for the SM sample to 466 and 842 MPa for the TM sample (Fig. 2h), respectively. Higher residual

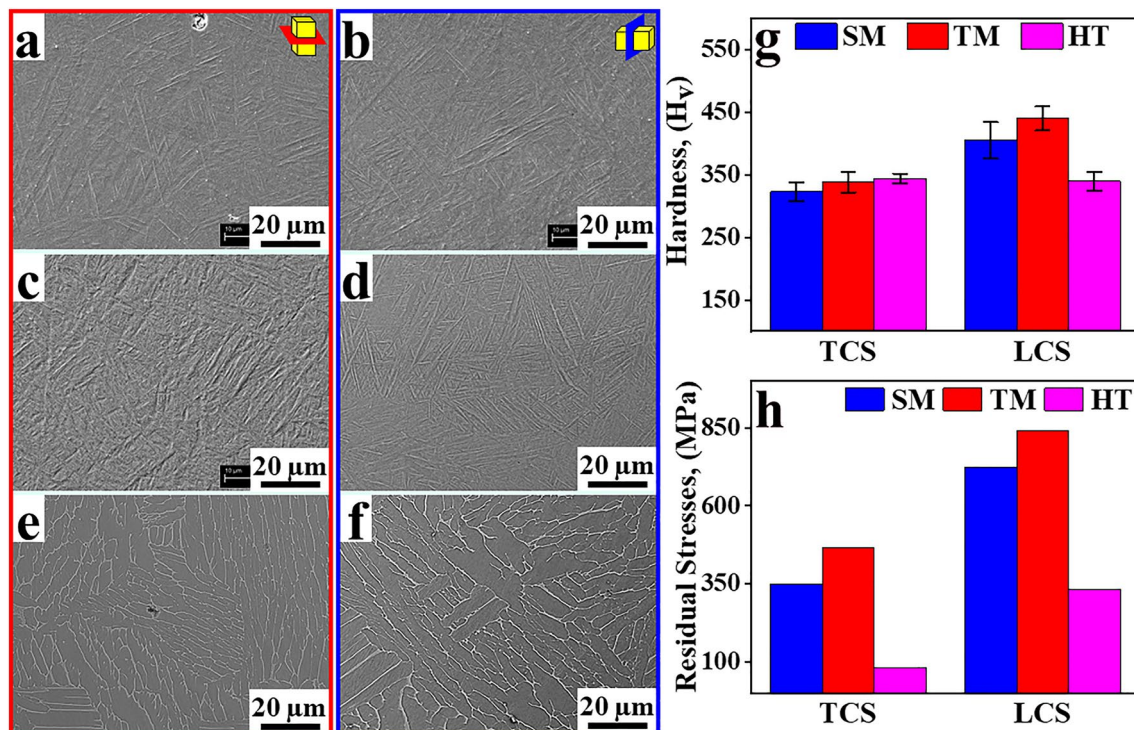


Fig. 2 SEM images of microstructure in TCS and LCS: SM a–b; TM c–d; and HT e–f. **g** Average hardness values and their distribution of the samples. **h** Residual stress values of the SLM and heat-treated samples in TCS and LCS

stress in the remelted SLM samples can be attributed to the significantly higher thermal conductivity of the bulk samples compared to the loose powder, in which this difference could be one order of magnitude (Casavola et al. 2008, Yilmaz and Kayacan 2021). Consequently, the cooling rate in the remelted SLM samples is higher than in as-built SLM samples. It can be seen that the residual stresses were considerably higher in the LCS than in TSC because of a higher temperature gradient and the formation of non-uniform anisotropic stress distribution. On the other hand, the HT sample showed a significant reduction in residual stresses in the TCS and LCS. Fang et al. (2020) reviewed the residual stress in the SLM components of different alloys and reported that residual stresses could be reduced by optimizing the SLM process parameters, pre-heating the powder particles and platform, post-processing (shot peening, laser finishing, etc.).

The compressive tests were carried out to evaluate the effect of the defects (like pores) in the SLM samples on the mechanical properties. The compressive properties are shown in Table 1, where it can be seen that the melting sequence improves the ultimate compressive strength (UCS) and yield compressive strength (YCS). Although the heat treatment process causes a decrease in the compressive strength, the fracture strain increases by 50%. Nevertheless, the compression strength of all the samples is higher than the values observed for the cast Ti6Al4V counterpart, as reported by Agrawal and Karthikeyan (2015). Our previous work described that the ultimate tensile strength and yield strength of the Ti6Al4V parts fabricated using the SLM process increased from the SM to the TM (Karimi et al. 2021a). In another work (Karimi 2022), we evaluated the effect of intrinsic defects (such as porosity) on the mechanical properties and observed an asymmetry in the strength behavior under tensile and compressive stress (strength differential effect). Furthermore, the chemical composition of the SLM and heat-treated samples were analyzed, indicating that there was no significant difference among the specimens, as shown in Table 1.

Hardness mapping of the additively manufactured parts was used as a tool to assess the inhomogeneity of

the hardness and understand the material behavior. The hardness distribution was quantified over the TCS and LCS surfaces of the SLM and heat-treated samples, as shown in Fig. 3a–c. The hardness distribution maps of the SM showed significant heterogeneity across the sample, where hardness ranges from ~ 200 to ~ 360 H_v for TCS and ~ 200 to ~ 480 H_v for LCS. However, the hardness maps of the TM sample showed a reduction in the heterogeneous distribution in the TCS and LCS. As observed in Fig. 2a–d, the morphology of the acicular α' changed, and λ decreased with the remelting scan strategy, which subsequently led to an increase in the hardness values and compressive strength, and homogenization of the TM sample. In addition, after the heat treatment process, the samples indicated a reduction of inhomogeneity and anisotropy in the hardness values.

The present results suggested that the remelting scan strategy mitigated the heterogeneity in the mechanical properties, enhanced the hardness value, and increased the compressive strength (UCS and YCS). The remelting scan strategy would be considered as a relatively low-cost and effective approach to overcome the SLM process shortcomings (such as heterogeneity in the mechanical properties) and improve productivity (like cutting the post-processing procedure). However, anisotropy in the mechanical properties remained in the SLM specimens, and the residual stresses increased by $\sim 25\%$ from the SM sample to the TM sample. The heat treatment process not only homogenized the hardness but also reduced the anisotropy in the mechanical properties and residual stresses. However, the heat treatment process decreased the UCS and YCS and increased the costs and time of the production process. Both approaches have their own pros and cons, and they can be applied depending on the required properties, possibility and performance, and the budget. Overall, it can be concluded that the remelting scan strategy and heat treatment process would be considered as the two potential approaches to overcome the shortcoming of the SLM process, where they will homogenize and refine the microstructure, and subsequently improve the mechanical properties of the SLM processed materials.

Table 1 Room-temperature compressive properties and chemical composition of the SLM and heat-treated samples

		Sample		
		SM	TM	HT
Compressive property	UCS, (MPa)	1404 ± 47	1526 ± 58	1314 ± 34
	YCS, (MPa)	1162 ± 181	1179 ± 47	933 ± 83
	Strain, (%)	22 ± 1	11 ± 2	24 ± 3
Chemical composition, (wt%)	Al	6.9	6.7	6.0
	V	2.7	4.0	4.0
	Fe	0.2	0.3	0.2
	Ti	Balance	Balance	Balance

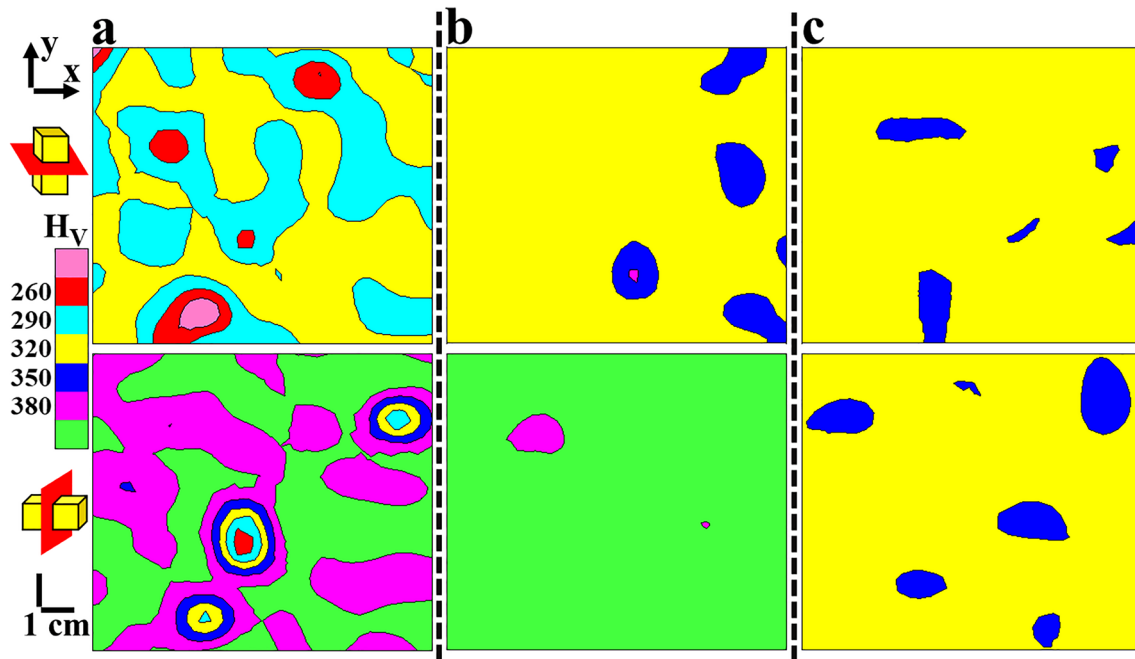


Fig. 3 Hardness distribution maps of the SLM samples in the TCS and LCS: **a** SM; **b** TM; and **c** HT

Summary

In the present study, the effect of the melting sequence and heat treatment approaches on the heterogeneity and anisotropy in microstructure and mechanical properties of the parts fabricated using the SLM process was studied and compared. The present results provided a considerable advance in the understanding of the effect of the melting sequence and heat treatment. The melting sequence strategy improved and homogenized the microstructure of the AM parts, though the anisotropy in mechanical properties remained, and residual stresses increased. However, the mechanical properties, including hardness and compressive strength (UCS and YCS), increased with the application of the melting sequence. On the other hand, heat treatment not only homogenized the hardness but also reduced the anisotropy and the residual stresses of the SLM samples. The present results open the door for overcoming the limitation of the SLM process with these approaches depending on the required properties, possibility and performance, and the budget.

Acknowledgements The authors would like to thank Ms. Laivi Väljaots and Mr. Rainer Traksmäa for their technical assistance.

Data availability The authors confirm that the data supporting the findings of this study are available within the article.

Declarations

Conflict of Interest No potential conflict of interest was reported by the authors.

References


- Agrawal P, Karthikeyan S (2015) Enhancement in strain hardening on boron addition in as-cast Ti–6Al–4V alloy. *Trans Indian Inst Met* 68:195–205. <https://doi.org/10.1007/s12666-015-0560-6>
- Ali H, Ma L, Ghadbeigi H, Mumtaz K (2017) In-situ residual stress reduction, martensitic decomposition and mechanical properties enhancement through high temperature powder bed pre-heating of selective laser melted Ti6Al4V. *Mater Sci Eng A* 695:211–220. <https://doi.org/10.1016/j.msea.2017.04.033>
- Ali H, Ghadbeigi H, Mumtaz K (2018) Effect of scanning strategies on residual stress and mechanical properties of Selective Laser Melted Ti6Al4V. *Mater Sci Eng A* 712:175–187. <https://doi.org/10.1016/j.msea.2017.11.103>
- Casavola C, Campanelli SL, Pappalettere C (2008) EXPERIMENTAL ANALYSIS OF RESIDUAL STRESSES IN THE SELECTIVE LASER MELTING PROCESS. Proceedings of the XIth International Congress and Exposition, June 2–5, Orlando, Florida USA.
- Fang ZC, Wu ZL, Huang CG, Wu CW (2020) Review on residual stress in selective laser melting additive manufacturing of alloy parts. *Opt Laser Technol* 129:106283. <https://doi.org/10.1016/j.optlastec.2020.106283>
- Fidan S, Avcu E, Karakulak E, Yamanoglu R, Zeren M, Sinmazcelik T (2013) Effect of heat treatment on erosive wear behaviour of

- Ti6Al4V alloy. *Mater Sci Technol* 29:1088–1094. <https://doi.org/10.1179/1743284713Y.0000000239>
- Karimi J, Ma P, Jia YD, Prashanth KG (2020) Linear patterning of high entropy alloy by additive manufacturing. *Manuf Lett* 24:9–13. <https://doi.org/10.1016/j.mfglet.2020.03.003>
- Karimi J, Suryanarayana C, Okulov I, Prashanth KG (2021a) Selective laser melting of Ti6Al4V: Effect of laser re-melting. *Mater Sci Eng A* 805:140558. <https://doi.org/10.1016/j.msea.2020.140558>
- Karimi J, Xie MS, Wang Z, Prashanth KG (2021b) Influence of sub-structures on the selective laser melted Ti-6Al-4V alloy as a function of laser re-melting. *J Manuf Process* 68:1387–1394. <https://doi.org/10.1016/j.jmapro.2021.06.059>
- Karimi J (2022) Microstructural Homogenisation of Selective Laser Melted Ti6Al4V and CoCrFeMnNi High-Entropy Alloys. Ph.D. Dissertation, Tallinn University of Technology, Estonia.
- Pantelejev L, Koutny D, Palousek D, Kaiser J (2016) Mechanical and microstructural properties of 2618 Al-Alloy processed by SLM remelting strategy. *Mater Sci Forum* 891:343–349. <https://doi.org/10.4028/www.scientific.net/MSF.891.343>
- Rahmani R, Antonov M, Kollo L (2019) Selective laser melting of diamond-containing or postnitrided materials intended for impact-abrasive conditions: Experimental and analytical study. *Adv Mater Sci Eng* 2019:4210762. <https://doi.org/10.1155/2019/4210762>
- Rahmani R, Antonov M, Brojan M (2020) Lightweight 3D printed Ti6Al4V-AlSi10Mg hybrid composite for impact resistance and armor. *Integr Med Res* 9:13842–13854. <https://doi.org/10.1016/j.jmrt.2020.09.108>
- Shiomi M, Osakada K, Nakamura K, Yamashita T, Abe F (2004) Residual stress within metallic model made by selective laser melting process. *CIRP Ann-Manuf Technol* 53:195–198. [https://doi.org/10.1016/S0007-8506\(07\)60677-5](https://doi.org/10.1016/S0007-8506(07)60677-5)
- Srinivasan D, Singh A, Reddy AS, Chatterjee K (2022) Microstructural study and mechanical characterisation of heat-treated direct metal laser sintered Ti6Al4V for biomedical applications. *Mater Technol* 37:260–271. <https://doi.org/10.1080/10667857.2020.1830566>
- Vaithilingam J, Goodridge RD, Hague RJM, Christie SDR, Edmondson S (2016) The effect of laser remelting on the surface chemistry of Ti6Al4V components fabricated by selective laser melting. *J Mater Process Technol* 232:1–8. <https://doi.org/10.1016/j.jmatp.rotec.2016.01.022>
- Vrancken B, Thijs L, Kruth JP, Van Humbeeck J (2012) Heat treatment of Ti6Al4V produced by selective laser melting: Microstructure and mechanical properties. *J Alloys Compd* 541:177–185. <https://doi.org/10.1016/j.jallcom.2012.07.022>
- Vrancken B, Cainb V, Knutsen R, Humbeeck JV (2014) Residual stress via the contour method in compact tension specimens produced via selective laser melting. *Scr Mater* 87:29–32. <https://doi.org/10.1016/j.scriptamat.2014.05.016>
- Wang M, Wu Y, Lu S, Chen T, Zhao Y, Chen H, Tang Z (2016) Fabrication and characterization of selective laser melting printed Ti-6Al-4V alloys subjected to heat treatment for customized implants design. *Prog Nat Sci Mater Int* 26:671–677. <https://doi.org/10.1016/j.pnsc.2016.12.006>
- Wu M, Lai P, Chen J (2016) Anisotropy in the impact toughness of selective laser melted Ti-6Al-4V alloy. *Mater Sci Eng A* 650:295–299. <https://doi.org/10.1016/j.msea.2015.10.045>
- Yasa E, Kruth JP (2011) Application of Laser Remelting on Selective Laser Melting Parts. *Adv Prod Eng Manag* 6:259–270
- Yilmaz N, Kayacan MY (2021) Effect of single and multiple parts manufacturing on temperature-induced residual stress problems in SLM. *Int J Mater Form* 14:407–419. <https://doi.org/10.1007/s12289-020-01560-1>
- Zheng Z, Jin X, Bai Y, Yang Y, Ni C, Lu WF, Wang H (2022) Microstructure and anisotropic mechanical properties of selective laser melted Ti6Al4V alloy under different scanning strategies. *Mater Sci Eng A* 831:142236. <https://doi.org/10.1016/j.msea.2021.142236>

Publisher's Note Springer Nature remains neutral with regard to jurisdictional claims in published maps and institutional affiliations.

Springer Nature or its licensor (e.g. a society or other partner) holds exclusive rights to this article under a publishing agreement with the author(s) or other rightsholder(s); author self-archiving of the accepted manuscript version of this article is solely governed by the terms of such publishing agreement and applicable law.

Authors and Affiliations

J. Karimi^{1,2}  · L. Kollo¹ · K. G. Prashanth^{1,3,4}

✉ J. Karimi
karimi@bias.de

¹ Department of Mechanical and Industrial Engineering, Tallinn University of Technology, Ehitajate tee 5, 19086 Tallinn, Estonia

² BIAS–Bremer Institut für angewandte Strahltechnik GmbH, Klagenfurter Straße 5, 28359 Bremen, Germany

³ Erich Schmid Institute of Materials Science, Austrian Academy of Sciences, Jahnstraße, 12, 8700 Leoben, Austria

⁴ CBCMT, School of Engineering, Vellore Institute of Technology, Vellore, Tamil Nadu 632014, India